

**Relationship between spring tropical cyclone frequency over the western North Pacific and El Niño-Southern Oscillation**

**Jinjie Song\*<sup>1</sup>, Philip J. Klotzbach<sup>2</sup> and Yihong Duan<sup>1</sup>**

<sup>1</sup> Chinese Academy of Meteorological Sciences, China

<sup>2</sup> Department of Atmospheric Science, Colorado State University, USA

**Submitted to**

*International Journal of Climatology*

**Second Revision**

\*Corresponding author: Jinjie Song

Address: 46 Zhongguancun South Avenue, Beijing, China, 100081

Email: [songjinjie@qq.com](mailto:songjinjie@qq.com)

**Keywords:** tropical cyclone, El Niño-Southern Oscillation, western North Pacific

**Funding information:** The National Natural Science Foundation of China (61827901 and 41575044), the National Key Research and Development Program of China

This article has been accepted for publication and undergone full peer review but has not been through the copyediting, typesetting, pagination and proofreading process which may lead to differences between this version and the Version of Record. Please cite this article as doi: 10.1002/joc.6703

(2018YFC1507305), the fifth period of 2019 “333 Project” in Jiangsu Province of China, and the G. Unger Vetlesen Foundation.

Accepted Article

## Abstract

The number of tropical cyclones (TCs) over the western North Pacific (WNP) during spring (March-May) has a significant inverse correlation with concurrent El Niño-Southern Oscillation (ENSO) conditions during the period from 1979-2018. This relationship is different from the previously-documented weak relationship between TC frequency and ENSO during the climatologically most active portion of the TC season. In general, TCs seldom occur in El Niño years during March-May, whereas they frequently form over the western part of the WNP, particularly to the southeast of the Philippines, in La Niña years. This difference can be largely explained by ENSO-driven differences in the genesis potential index as derived from environmental variables. In La Niña years, the abnormally moist mid-troposphere, which relates to the strengthened vertical transport of water vapor induced by the enhanced Walker Circulation, primarily favors TC development, while increased sea surface temperatures and positive low-level relative vorticity anomalies appear to play a lesser role in impacting TC formation.

## 1 Introduction

Tropical cyclones (TCs) are among the most devastating natural disasters on Earth, posing a significant threat to various coastal regions. Increasing attention has been paid to the temporal variability in TC activity for all TC basins in recent years, especially as concerns about climate change's impacts escalate (Walsh et al., 2016). The western North Pacific (WNP) is the most active basin for TC formation across the world on an annually-averaged basis, with around one-third of global TCs occurring in the WNP basin, on average (Lee et al., 2012). The active season for WNP TCs is usually defined to extend from June to November (Neumann, 1993), which approximately refers to the 5th to 95th percentile of climatological TC genesis dates (Kim et al., 2017). Therefore a large number of previous publications have investigated changes in TC activity over the WNP during boreal summer and autumn (e.g. Chen et al., 1998; Camargo and Sobel, 2005). Furthermore, the WNP is the only basin with at least one TC occurring in every calendar month, with TCs forming fairly often even during off-season months (Ramsay, 2017). For instance, Typhoon Mitag, which developed near the Federal States of Micronesia in 2002, was the first instance of a TC reaching super typhoon strength in March (Ramsay, 2017). However, the features related to variations in WNP TC activity are seldom investigated during the climatologically inactive seasons, e.g., the boreal winter or spring.

Tu et al. (2011) reported a sudden increase in the number of intense WNP typhoons in May after 2000, which primarily resulted from increased tropospheric water vapor. Xu and Wang (2014) further noted that there was a sharp increase in the power dissipation index (PDI) of WNP TCs during May from 1979-1999 to 2000-2011. Larger PDI in May after 2000 was induced by both greater TC frequency, consistent with a significant increase in the genesis potential index and higher TC intensity that was linked to both increased maximum potential intensity and reduced

vertical wind shear (Xu and Wang, 2014). In addition, Huangfu et al. (2017) ascribed the abrupt increase in WNP TC frequency during May to an earlier onset of the South China Sea (SCS) summer monsoon in 1999-2013 than in 1979-1998. This was a result of the monsoon trough, which is known to facilitate TC development, moving into the WNP earlier. Despite the aforementioned interdecadal increase in TC frequency during May, the characteristics of interannual variation in TC activity over the WNP during the boreal spring are not well known.

It is now well accepted that El Niño-Southern Oscillation (ENSO) modulates the interannual variability of TC activity over the WNP (e.g. Chan, 1985; Lander, 1994; Chan 2000; Saunders et al., 2000; Wang and Chan, 2002; Wu et al., 2004; Zhao et al., 2010; Kim et al., 2011; Li and Zhou, 2012; Patricola et al., 2018; Zhao and Wang, 2019). These studies have generally found only a weak correlation between ENSO and total TC count over the entire WNP, while the migration of the average location of TC formation is significantly influenced by ENSO. The mean TC genesis location shifts farther eastward and equatorward during El Niño years relative to La Niña years, due to anomalously warm sea surface temperatures (SSTs), higher relative humidity, lower vertical wind shear (VWS) and weaker trade winds in the southeastern quadrant of the WNP. This displacement implies longer tracks for TCs developing over the warm waters of the tropical WNP, allowing these TCs to achieve a greater lifetime maximum intensity (LMI) during El Niño years than during La Niña years. Consequently, this increases not only the number of intense TCs but also the accumulated cyclone energy (ACE) generated by TCs during El Niño years relative to La Niña years (Patricola et al. 2018). Nonetheless, the general consensus is predominantly established based on the influence of ENSO on TC activity during the climatologically active TC season, or over the entire year which includes the majority of TCs which occur in summer and autumn. It is still unclear whether ENSO has an

Accepted Article

impact on WNP TC activity when only the spring is considered, or whether the mechanisms of large-scale environmental variables influencing summertime WNP TC activity work in a similar fashion in the spring.

The primary objectives of this study are to investigate the potential relationship between spring TC frequency over the WNP and concurrent ENSO conditions. The remainder of this paper is organized as follows. The data and methodology are briefly described in Section 2. The differences in the features of spring WNP TC formation during different ENSO phases are provided in Section 3. A possible mechanism for the influence of ENSO on spring WNP TC genesis is explained in Section 4. A summary of this work is given in the last section.

## 2 Data and methodology

TC best track data used in this study are from the Joint Typhoon Warning Center (JTWC), including TC center location and intensity at a 6-h interval, which are compiled in the International Best Track Archive for Climate Stewardship (IBTrACS) v04r00 (Knapp et al., 2010). Because of the relatively low quality of the best track data prior to the late 1970s (Chu et al., 2002), TC data between 1979 and 2018 are investigated here. To reduce the uncertainty in detecting weak TCs such as tropical depressions (Klotzbach and Landsea, 2015), we only consider TCs with LMIs of at least 34 kt (e.g., named storms). TC genesis is defined as the first record when a TC was listed in the JTWC dataset, while spring TCs refer to TCs forming in March, April and May.

Monthly mean SST data over a  $2^{\circ} \times 2^{\circ}$  grid are provided by the National Oceanic and Atmospheric Administration (NOAA) Extended Reconstructed SST v5 (Huang et al., 2017). Monthly mean atmospheric data are obtained from the Fifth generation of the European Centre for Medium-Range Weather Forecasts (ECMWF) atmospheric

Accepted Article

reanalyses (ERA5; C3S, 2017). The original atmospheric fields with a resolution of  $0.25^{\circ} \times 0.25^{\circ}$  are converted to a  $2^{\circ} \times 2^{\circ}$  grid for calculating the genesis potential index (GPI; Emanuel and Nolan, 2004). Monthly interpolated outgoing longwave radiation (OLR) data at a  $2.5^{\circ} \times 2.5^{\circ}$  grid (Liebmann and Smith, 1996) are from NOAA's Climate Diagnostics Center. The temporal variation in ENSO is measured by the monthly Multivariate ENSO Index (MEI) v2 (Zhang et al., 2019), which considers five different ENSO-related variables (sea level pressure, SST, zonal and meridional surface winds, and OLR) over the tropical Pacific. During the period from 1979-2018, El Niño and La Niña years refer to the seven March-May (e.g., spring) periods with the highest and lowest MEI values, respectively.

The significance levels ( $p$ ) of the correlation coefficients are estimated based on a two-tailed Student's  $t$ -test. The significance levels for differences in the averages of the two samples are based on a two-tailed paired sample  $t$ -test.

### 3 Relationship between spring WNP TC Frequency and ENSO

Figure 1a shows the annual variation of spring TC frequency over the WNP from 1979 to 2018. Around 2.4 WNP TCs occur, on average, during the spring each year, accounting for 9% of all WNP TCs. There are five years without spring TC formation, with four of them corresponding to El Niño years. Figure 1a further displays an inverse relationship between WNP TC frequency and the MEI during the spring ( $r = -0.38$ ;  $p = 0.02$ ), implying that El Niño suppresses and La Niña favors spring TC genesis over the WNP. Note that this relationship is different from that experienced during the TC-active portion of the season (e.g. Zhang and Wang, 2019). On average, the annual numbers of spring TCs are 0.6 and 2.9 in El Niño and La Niña years, respectively (Table 1). This difference of 2.3 TCs is significant ( $p < 0.01$ ). Figure 1b-d further represents the annual WNP TC frequencies during the individual months of March,

Accepted Article

April and May, which account for 20%, 27% and 53% of spring TCs, respectively. During March and April, there are small and insignificant correlations of -0.02 ( $p=0.92$ ) and -0.13 ( $p=0.42$ ), respectively between TC number and the MEI, indicating a minor impact of ENSO on TC formation. In contrast, there is a significant relationship between TC frequency and the MEI during May ( $r=-0.34$ ;  $p=0.03$ ). This significant correlation in May is primarily responsible for the significant correlation obtained during the spring between TC frequency and the MEI, given that May TCs comprise more than half of all spring TCs.

In addition to TC frequency, there are also substantial differences in the genesis location for spring TCs based on ENSO phase (Figure 2a). In El Niño years since 1979, only four TCs have formed during the spring. All of these TCs developed in the southeastern corner of the WNP ( $0^{\circ}\sim 10^{\circ}\text{N}$ ,  $150^{\circ}\text{E}\sim 180^{\circ}$ ), which is farther southeast than the region favorable for TC formation during the climatologically most active portion of the TC season (e.g.  $0^{\circ}\sim 15^{\circ}\text{N}$ ,  $140^{\circ}\text{E}\sim 180^{\circ}$ ; Li and Zhou, 2012). In La Niña years, a large number of spring TCs occur west of  $150^{\circ}\text{E}$  over the tropical WNP, with the most frequent region for spring TC formation being southeast of the Philippines ( $5^{\circ}\sim 10^{\circ}\text{N}$ ,  $130^{\circ}\sim 140^{\circ}\text{E}$ ). The distribution of TC genesis locations is captured to a great extent by the pattern of the GPI difference between different ENSO years (Figure 2b), indicating that the differences in the spatial distribution of spring TC formation primarily result from different large-scale environments in El Niño and La Niña years. There are positive GPI differences west of  $150^{\circ}\text{E}$  over the WNP, with the largest differences corresponding well with the region where TCs occur more frequently in La Niña years. This region is bounded by the green dashed line in Figure 1c and is referred to as the main development region (MDR) hereafter. In comparison, the negative GPI difference is shifted slightly eastward compared with the region where TC formation occurs in El Niño years.



Accepted Article

During all three months of the spring, WNP TCs generally occur more westward in La Niña years than in El Niño years, despite no March TCs forming westward of 140°E (Figure 2c, e, g). Although the annual TC frequency is not significantly correlated with the MEI during March and April, the spatial pattern of TC formation in El Niño and La Niña years exhibits similar features to the genesis distribution of May TCs. Moreover, the spatial distributions of the GPI differences in individual months are consistent with that for the entire spring, showing a large-scale environment enhancing TC occurrences west of 150°E and suppressing TC occurrences east of 150°E in La Niña years (Figure 2d, f, h). The positive GPI difference southeast of the Philippines is the largest in May, roughly corresponding to where the greatest number of TCs form in May during La Niña years. There are no large discrepancies between the distribution of TC occurrence and large-scale environmental variables relevant to TC development in March, April or May.

#### **4 Mechanism for ENSO's modulation of spring WNP TC formation**

Since the number of spring TCs in El Niño years (Table 1) is not significantly different from zero ( $p=0.10$ ), we will primarily explain why there are more spring TCs forming over the MDR in La Niña years than in El Niño years. Figure 3 displays the differences in the variables constituting the GPI between different ENSO phases. In La Niña years, there are significantly higher SSTs extending from the tropical central WNP to the subtropical central Pacific, while there are significantly lower SSTs over the tropical central Pacific (Figure 3a). Warmer SSTs are favorable for spring TC genesis over the eastern part of the MDR (east of 130°E). In comparison, there are significant differences in 600-hPa relative humidity (RH600) over the entire MDR, with RH600 in La Niña years at least 10% larger than in El Niño years over a large portion of the WNP (Figure 3b). TCs are more likely to develop with a moister mid-

troposphere over the MDR in La Niña years.

In addition to the thermodynamic variables, there are also some differences in dynamic parameters between El Niño and La Niña years. Figure 3c displays significant cyclonic anomalies in 850-hPa relative vorticity (VOR850) over the western part of the WNP, with the two regions where the largest differences occur over the SCS and the southern Philippines. Anomalous low-level cyclonic vorticity is beneficial for spring TC formation over the western part of the MDR (west of 130°E) in La Niña years. In addition, there are generally positive and negative differences in 850-200-hPa vertical wind shear (VWS) south and north of 10°N, respectively (Figure 3d). Although VWS in La Niña years is lower than in El Niño years over almost all of the entire MDR, significant decreases in VWS only exist over the northwestern and northeastern corners of the MDR. Consequently, it appears that VWS changes are only a minor contributor to ENSO's modulation of spring WNP TC formation.

To summarize, spring WNP TC genesis is primarily modulated by differences in mid-level moisture between different ENSO phases, with other large-scale variables having only minor impacts on changes in spring WNP TC formation. Figure 4 illustrates how the spring phase of ENSO modulates WNP TC genesis. As found in prior research (e.g. Wallace et al., 1998; Wang et al., 2000), there are cooler SSTs over the central and eastern Pacific and warmer SSTs in the western Pacific in La Niña years relative to El Niño years, accompanied by anomalous easterlies over the central Pacific (Figure 4a). Associated with these SST anomalies is a strengthened Walker Circulation in La Niña years, with enhanced upward motion over the Philippine Sea and anomalous westerlies over southeast Asia, favoring vertical transport of water vapor from the underlying sea and horizontal transport of moisture from the Indian Ocean, which both lead to an increase in mid-level moisture (Figure 4b). As shown by the anomalously low OLR east of the Philippines (Figure 4c), the stronger updrafts

associated with the moister atmosphere result in enhanced convection in La Niña years, increasing the probability for TC formation. Moreover, the enhanced convective heating east of the Philippines also generates a cyclonic low-level circulation that is favorable for TC development (Figure 4a).

## 5 Summary

The modulation of ENSO on the formation of spring (March-May) WNP TCs is investigated in this study. There is a significant inverse relationship between the variation in spring TC frequency (as well as May individually) and the concurrent MEI during 1979-2018, indicating that El Niño generally suppresses and La Niña favors WNP TC development during the spring. During the full spring and each of its component months (e.g., March, April and May), WNP TCs predominantly form over the southeastern corner of the WNP in El Niño years, whereas they primarily generate over the western part of the WNP in La Niña years. The most frequent formation region for spring TCs in La Niña years is southeast of the Philippines in the MDR. Note that the preferential genesis locations for spring WNP TCs between different ENSO phases is well separated (Figure 2).

The spatial difference in spring WNP TC genesis between El Niño and La Niña years, which is well captured by the distribution of the GPI difference, is linked to the differences in large-scale environmental variables. The distributions of the GPI differences share similar patterns in each of the three spring months. During the springs of La Niña years, there is increased SST and VOR850 over the eastern and western halves of the MDR, respectively, while the mid-troposphere is significantly moister over the entire MDR relative to El Niño years. Lastly, we propose that during the spring, the enhanced Walker Circulation in La Niña years increases upward motion over the MDR as well as westerlies over southeast Asia, thereby strengthening

the vertical transport of water vapor from the underlying sea and eastward transport of moisture for the Indian Ocean, which both subsequently enhance convection that is favorable for TC development. Although previous studies have reported that mid-level relative humidity and low-level vorticity are both important for changes in summertime TC genesis related to ENSO over the WNP (e.g. Camargo et al., 2007), our results show that differences in mid-level relative humidity are the primary factor causing ENSO-driven changes in TC formation during the spring.

## References

- Camargo, S. J., & A. H. Sobel (2005). Western North Pacific tropical cyclone intensity and ENSO. *J. Clim.*, *18*, 2996–3006.
- Camargo, S. J., K. Emanuel, & A. H. Sobel (2007). Use of a genesis potential index to diagnose ENSO effects on tropical cyclone genesis. *J. Clim.*, *20*, 4819–4834.
- Chan, J. C. L. (1985). Tropical cyclone activity in the northwest Pacific in relation to the El Niño/Southern Oscillation phenomenon. *Mon. Wea. Rev.*, *113*, 599–606.
- Chan, J. C. L. (2000). Tropical cyclone activity over the western North Pacific associated with El Niño and La Niña events. *J. Clim.*, *13*, 2960–2972.
- Chen, T. C., S. P. Weng, N. Yamazaki, & S. Kiehne (1998). Interannual variation in the tropical cyclone formation over the western North Pacific. *Mon. Wea. Rev.*, *126*, 1080-1090.
- Chu, J.-H., C. R. Sampson, A. S. Levine, & E. Fukada (2002). The Joint Typhoon Warming Center tropical cyclone best-tracks, 1945-2000. *NRL Tech. Rep.* NRL/MR/7540-02-16, 22 pp.
- Copernicus Climate Change Service (C3S) (2017). ERA5: Fifth generation of ECMWF atmospheric reanalyses of the global climate. *Copernicus Climate Change Service Climate Data Store (CDS)*, available at <https://cds.climate.copernicus.eu/cdsapp#!/home>.
- Emanuel, K. A., & D. S. Nolan (2004). Tropical cyclone activity and global climate. Preprints, *26th Conf. on Hurricanes and Tropical Meteorology*, Miami, FL, Amer. Meteor. Soc., 240–241.
- Huang, B., & Coauthors (2017). Extended Reconstructed Sea Surface Temperature version 5 (ERSSTv5): Upgrades, validations, and intercomparisons. *J. Clim.*, *30*, 8179–8205.
- Kim, D., H. -S. Kim, D. - S. R. Park, & M. - S. Park (2017). Variation of the

tropical cyclone season start in the western North Pacific. *J. Clim.*, 30, 3297–3302.

Kim, H.-M., P. J. Webster, & J. A. Curry (2011) Modulation of North Pacific tropical cyclone activity by three phases of ENSO. *J. Clim.*, 24, 1839–1849.

Klotzbach, P. J., & C. W. Landsea (2015). Extremely intense hurricanes: Revisiting Webster et al. (2005) after 10 years. *J. Clim.*, 28, 7621-7629.

Knapp, K. R., M. C. Kruk, D. H. Levinson, H. J. Diamond, & C. J. Neuman (2010). The International Best Track Archive for Climate Stewardship (IBTrACS). *Bull. Amer. Meteor. Soc.*, 91, 363–376.

Lander, M. A. (1994). An exploratory analysis of the relationship between tropical storm formation in the western North Pacific and ENSO. *Mon. Wea. Rev.*, 122, 636-651.

Lee, T.-C., T. R. Knutson, H. Kamahori, & M. Ying (2012) Impacts of climate change on tropical cyclones in the western North Pacific basin. Part I: Past observations. *Trop. Cyclone Res. Rev.*, 1, 213–230.

Li, R. C. Y., & W. Zhou (2012). Changes in western Pacific tropical cyclones associated with the El Niño–Southern Oscillation cycle. *J. Clim.*, 25, 5864–5878.

Liebmann, B., & C. A. Smith (1996). Description of a complete (interpolated) outgoing longwave radiation dataset. *Bull. Amer. Meteor. Soc.*, 77, 1275–1277.

Neumann, C. J. (1993). Global overview. *Global Guide to Tropical Cyclone Forecasting*, World Meteor. Org., 1.1–1.56.

Patricola, C. M., S. J. Camargo, P. J. Klotzbach, R. Saravanan, & P. Chang (2018). The influence of ENSO flavors on western North Pacific tropical cyclone activity. *J. Clim.*, 31, 5395–5416.

Ramsay, H. A. (2017). The global climatology of tropical cyclones. *Oxford Research Encyclopedia of Natural Hazard Science*.

- Saunders, M. A., R. E. Chandler, C. J. Merchant, & F. P. Roberts (2000). Atlantic hurricanes and NW Pacific typhoons: ENSO spatial impacts on occurrence and landfall. *Geophys. Res. Lett.*, *27*, 1147–1150.
- Tu, J. Y., C. Chou, P. Huang, & R. Huang (2011). An abrupt increase of intense typhoons over the western North Pacific in early summer. *Environ. Res. Lett.*, *6*, 034013.
- Wallace, J. M., E. M. Rasmusson, T. P. Mitchell, V. E. Kousky, E. S. Sarachik, & H. von Storch (1998). On the structure and evolution of ENSO-related climate variability in the tropical Pacific: Lessons from TOGA. *J. Geophys. Res.*, *103*, 14241–14260.
- Walsh, K. J. E., & Coauthors (2016). Tropical cyclones and climate change. *Wiley Interdiscip. Rev.: Climate Change*, *7*, 65–89.
- Wang, B., R. Wu, & X. Fu (2000). Pacific–East Asian teleconnection: How does ENSO affect east Asian climate. *J. Clim.*, *13*, 1517–1536.
- Wang, B., & J. C. L. Chan (2002). How strong ENSO events affect tropical storm activity over the western North Pacific. *J. Clim.*, *15*, 1643–1658.
- Wu, M. C., W. L. Chang, & W. M. Leung (2004). Impacts of El Niño–Southern Oscillation events on tropical cyclone landfalling activity in the western North Pacific. *J. Clim.*, *17*, 1419–1428.
- Xu, S., & B. Wang (2014). Enhanced western North Pacific tropical cyclone activity in May in recent years. *Clim. Dyn.*, *42*, 2555–2563.
- Zhang, T, A. Hoell, J. Perlwitz, J. Eischeid, D. Murray, M. Hoerling & T. Hamill (2019). Towards Probabilistic Multivariate ENSO Monitoring, *Geophys. Res. Lett.*, *46*, 10532–10540.
- Zhao, H., L. Wu, & W. Zhou (2010). Assessing the influence of the ENSO on tropical cyclone prevailing tracks in the western North Pacific. *Adv. Atmos. Sci.*, *27*,

1361–1371.

Zhao, H., & C. Wang (2019). On the relationship between ENSO and tropical cyclones in the western North Pacific during the boreal summer. *Clim. Dyn.*, 52, 275-288.

Accepted Article



## Acknowledgements

We would like to express our sincere thanks to two anonymous reviewers for their helpful comments on an earlier version of this manuscript. This work was jointly funded by the National Natural Science Foundation of China (61827901), the National Key Research and Development Program of China (2018YFC1507305), the National Natural Science Foundation of China (41575044) and the fifth period of 2019 “333 Project” in Jiangsu Province of China. Klotzbach would like to acknowledge financial support from the G. Unger Vetlesen Foundation.

## Figure captions

**Figure 1.** Time series of WNP TC number and the MEI during 1979-2018 for (a) spring (March, April and May), (b) March, (c) April and (d) May. In (a), red squares and blue triangles refer to the seven highest and lowest MEI years (El Niño and La Niña years), respectively.

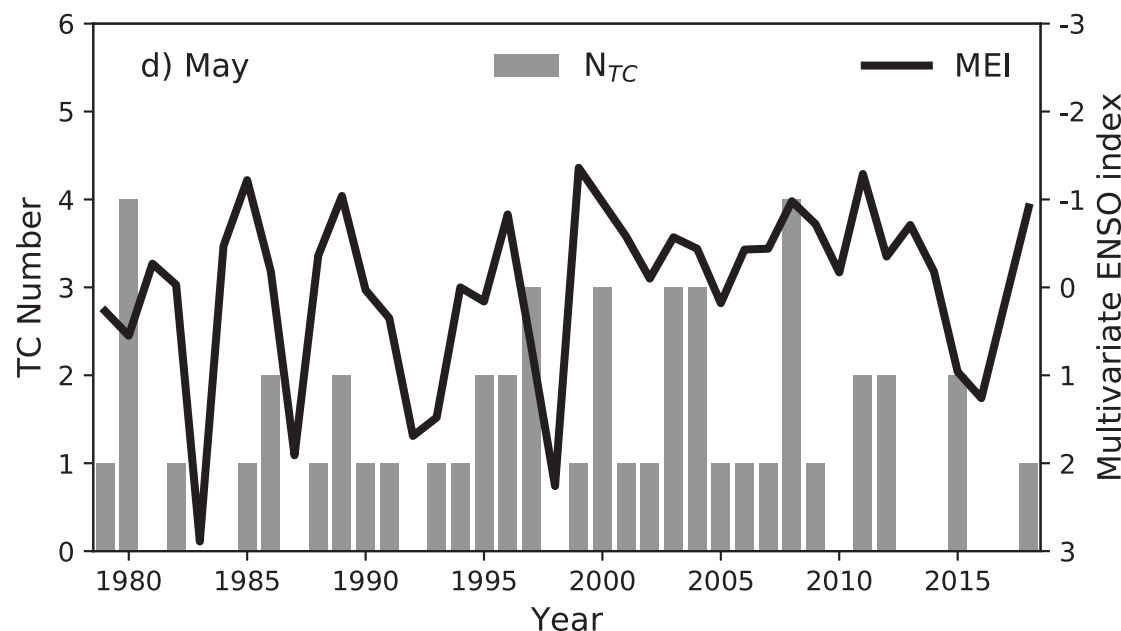
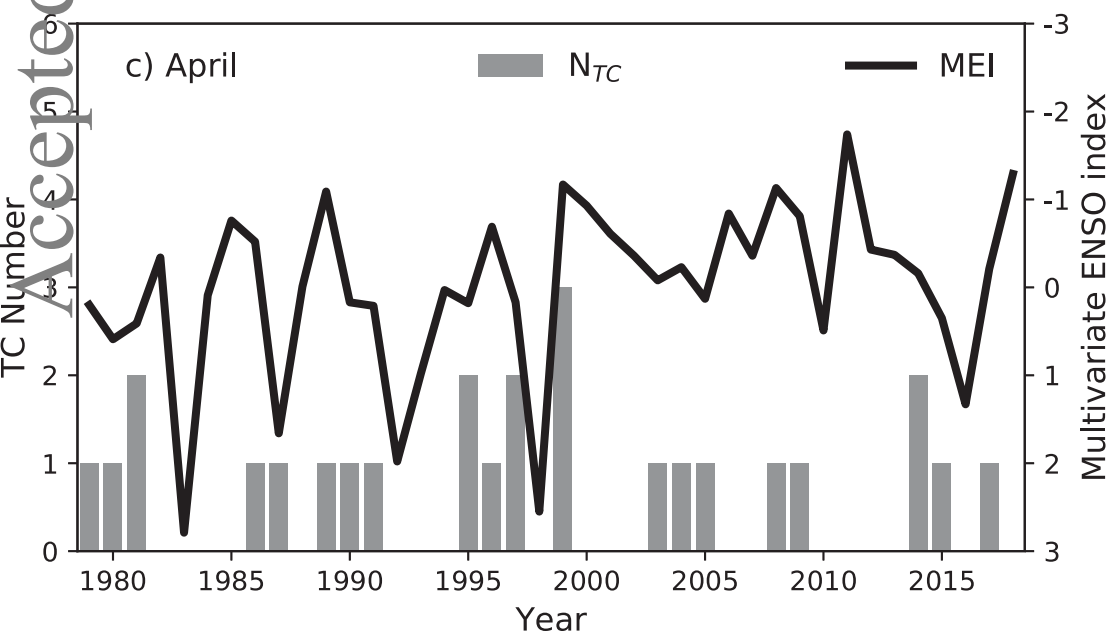
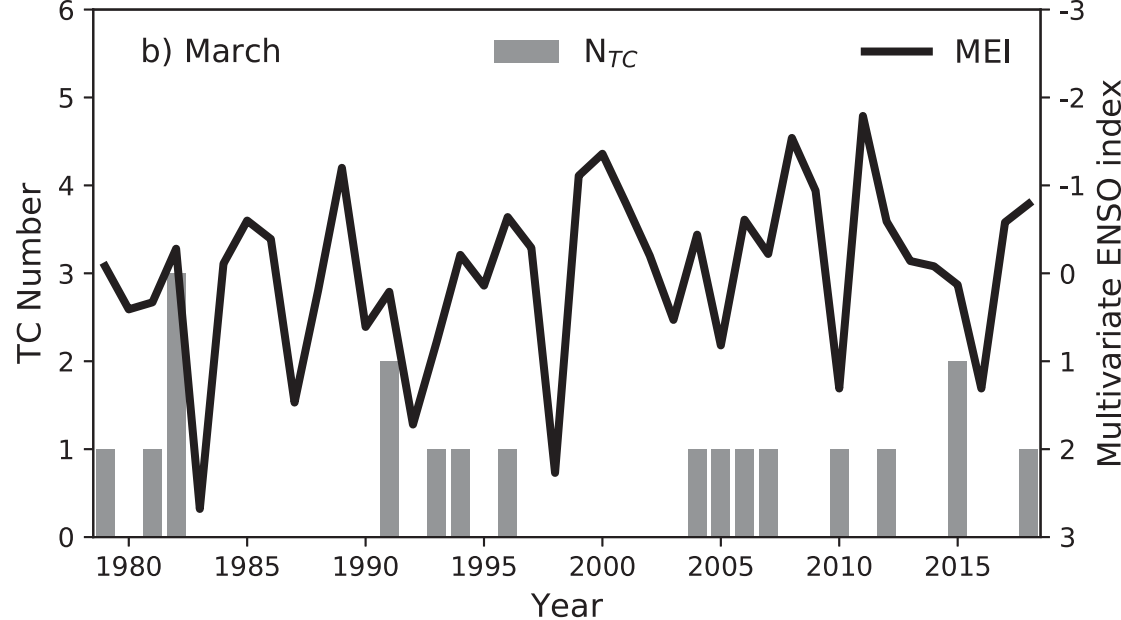
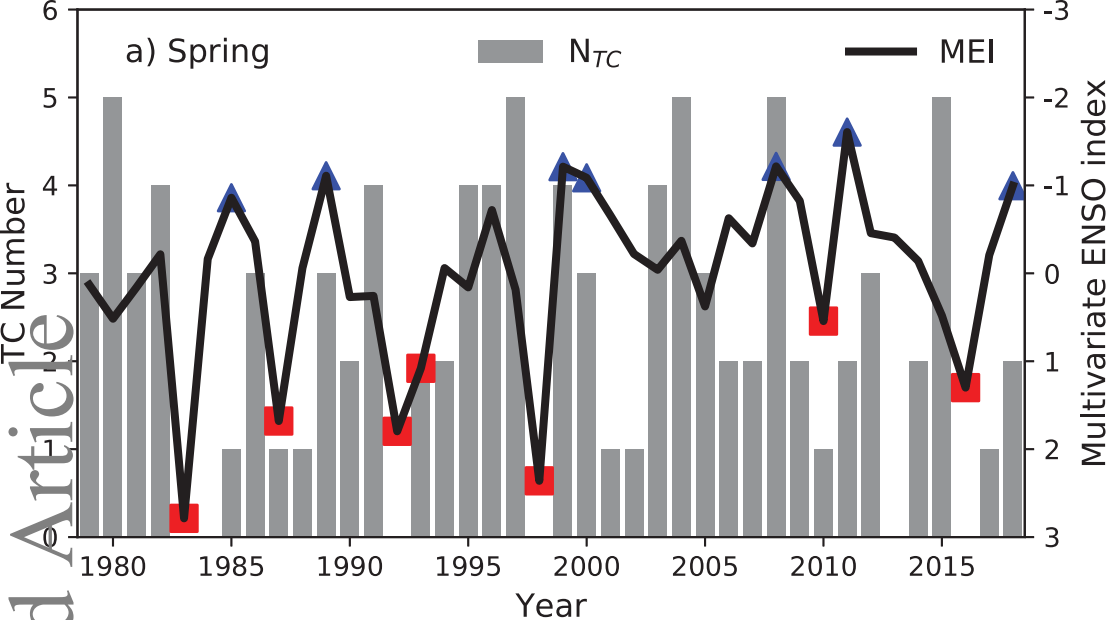
**Figure 2.** TC genesis locations during the two ENSO phases and GPI differences between El Niño and La Niña years for (a, b) spring, (c, d) March, (e, f) April and (g, h) May, respectively. In (a, c, e and g), red squares and blue triangles denote El Niño and La Niña seasons, respectively. In (b, d, f and h), black crosses refer to differences significant at the 0.05 level based on a Student's *t*-test. Green dashed lines in (a) indicate the total occurrence number over a  $5^\circ \times 5^\circ$  grid in La Niña years, while the green dashed lines in other panels denote the area with at least three TCs forming in La Niña years. This area is referred to as the main development region (MDR) throughout the remainder of the text.

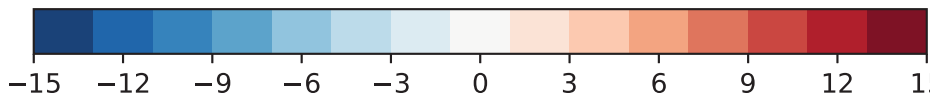
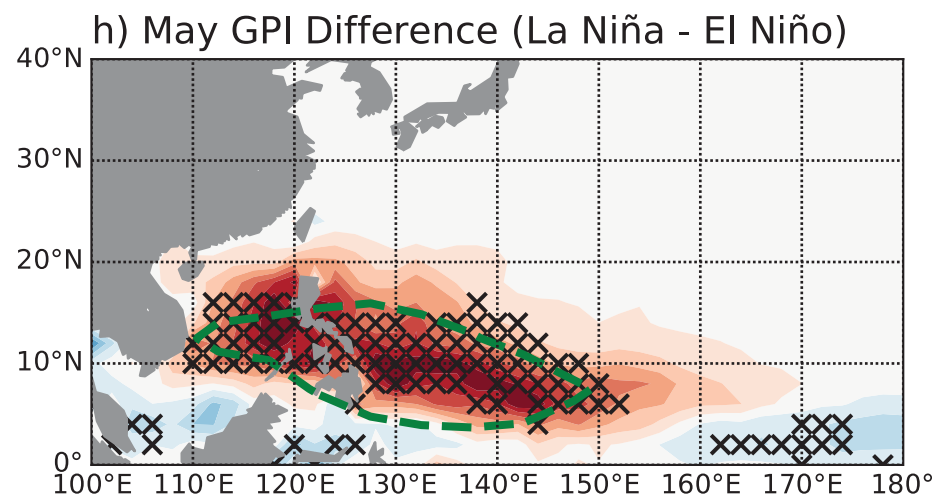
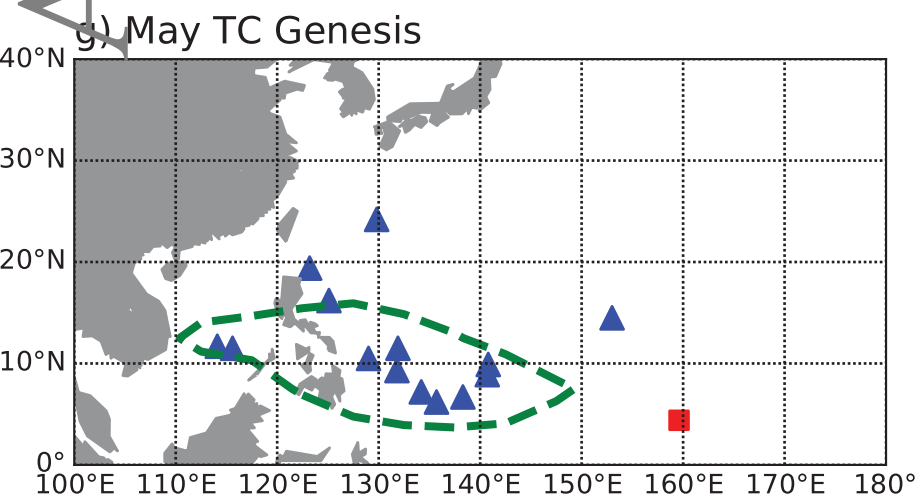
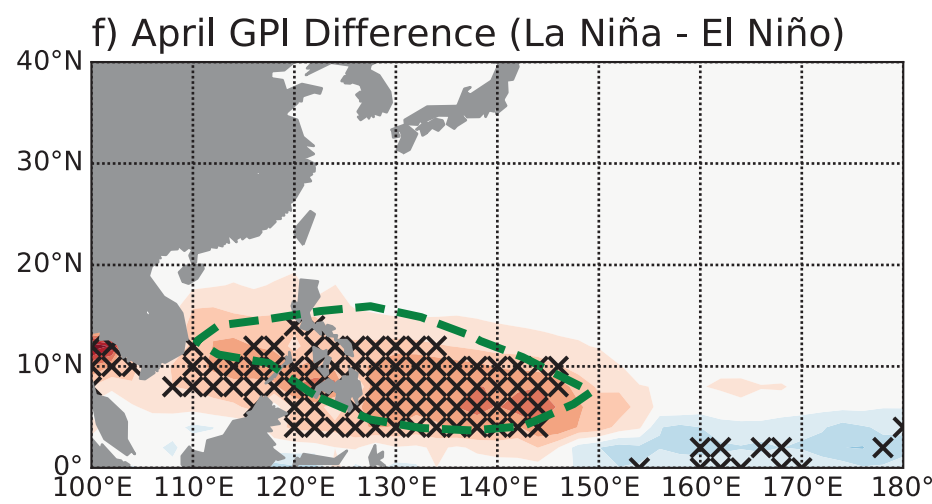
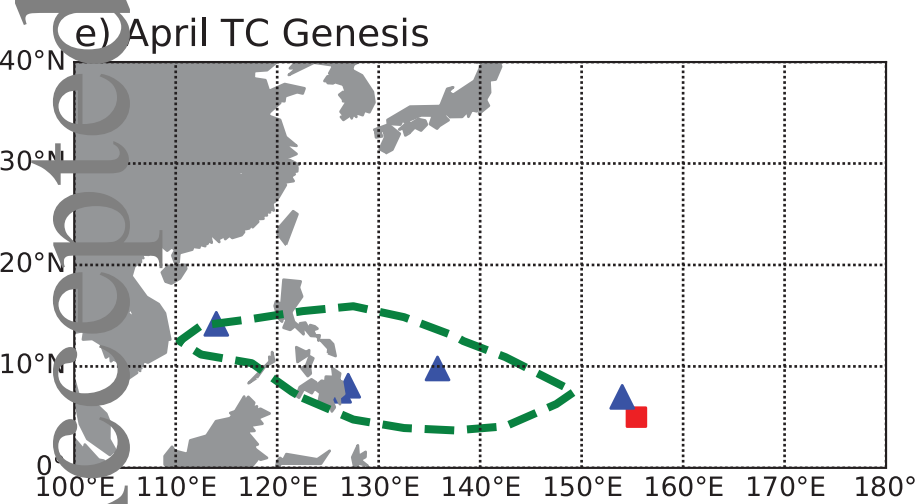
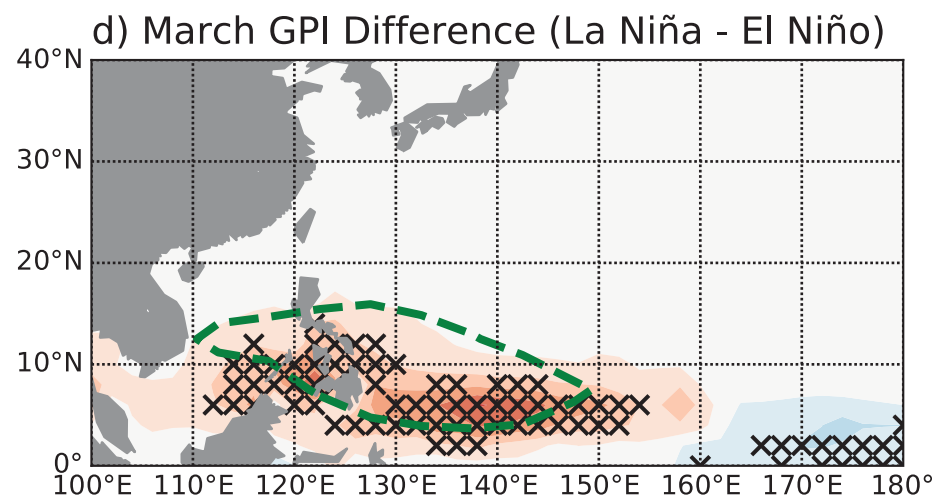
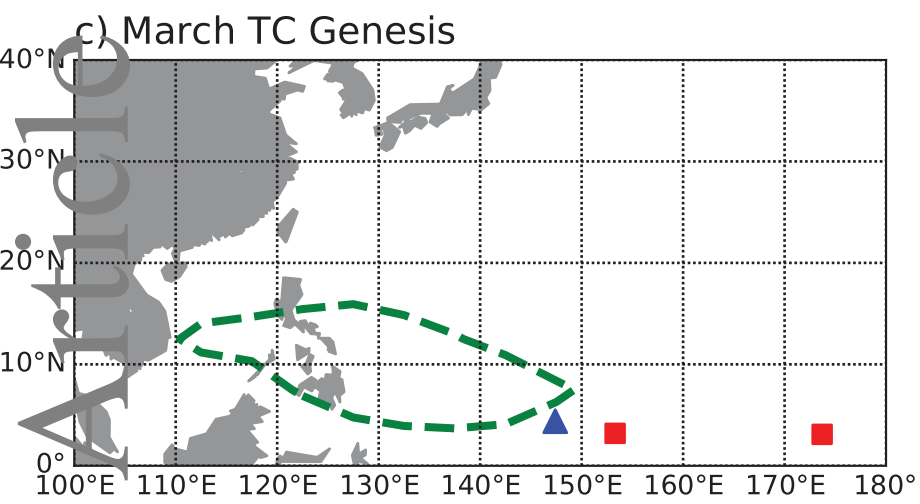
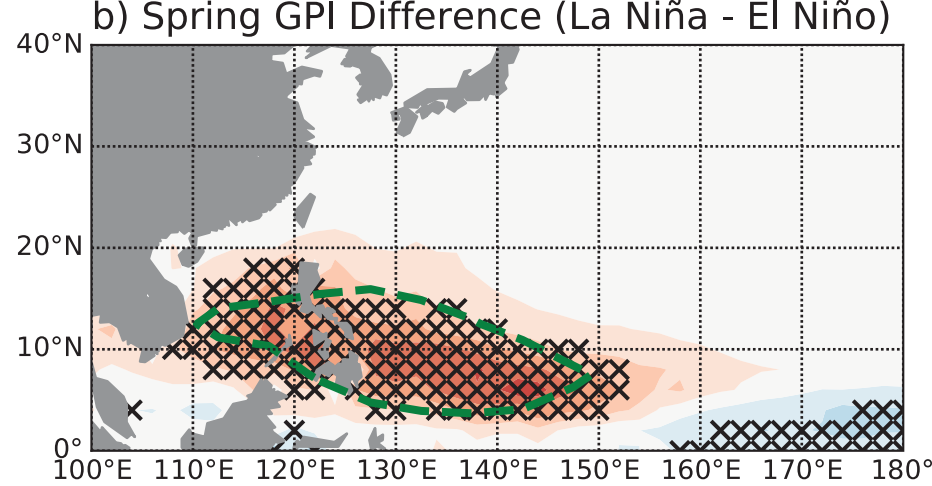
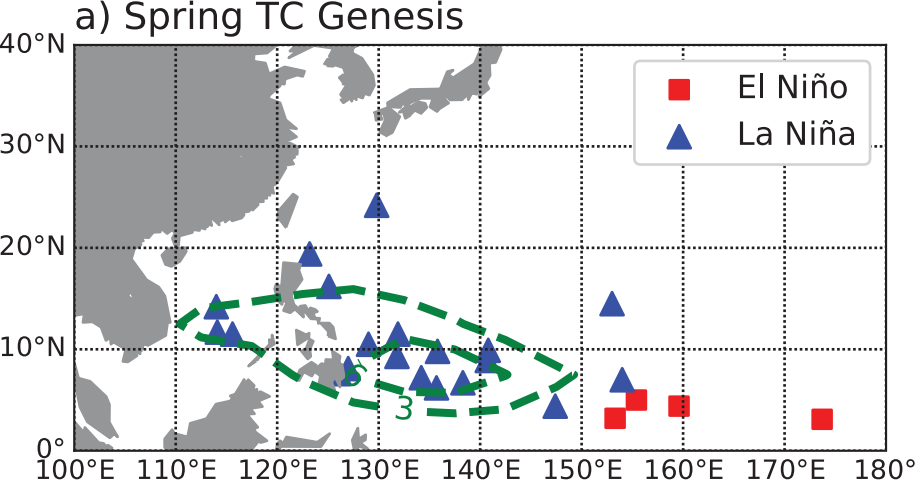
**Figure 3.** La Niña minus El Niño differences in environmental variables during March-May over the western North Pacific. (a) Sea surface temperature ( $^\circ\text{C}$ ), (b) 600-hPa relative humidity (%), (c) 850-hPa relative vorticity ( $\times 10^{-6} \text{ s}^{-1}$ ) and (d) 850-200-hPa vertical wind shear ( $\text{m s}^{-1}$ ). Differences significant at the 0.05 level are represented with black crosses.

**Figure 4.** La Niña minus El Niño differences in the large-scale environment during March-May over the Indian/Pacific Oceans. (a) Sea surface temperature (shaded;  $^\circ\text{C}$ ) and 850-hPa wind streamlines. (b) 500-hPa vertical velocity (shaded;  $10^{-2} \text{ Pa s}^{-1}$ ) and 600-hPa specific humidity (contours;  $\text{g kg}^{-1}$ ) and (c) outgoing longwave radiation (shaded;  $\text{W m}^{-2}$ ) and 200-hPa wind streamlines.

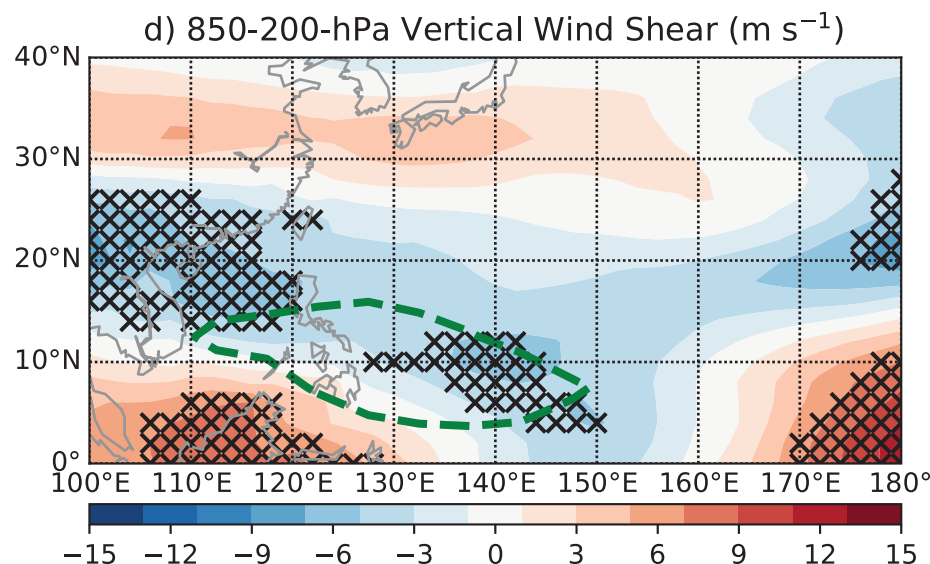
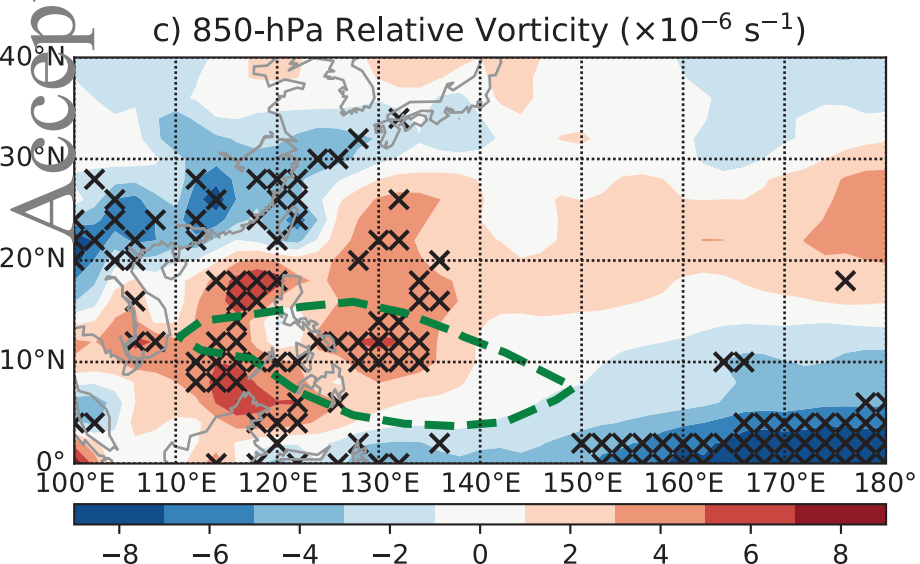
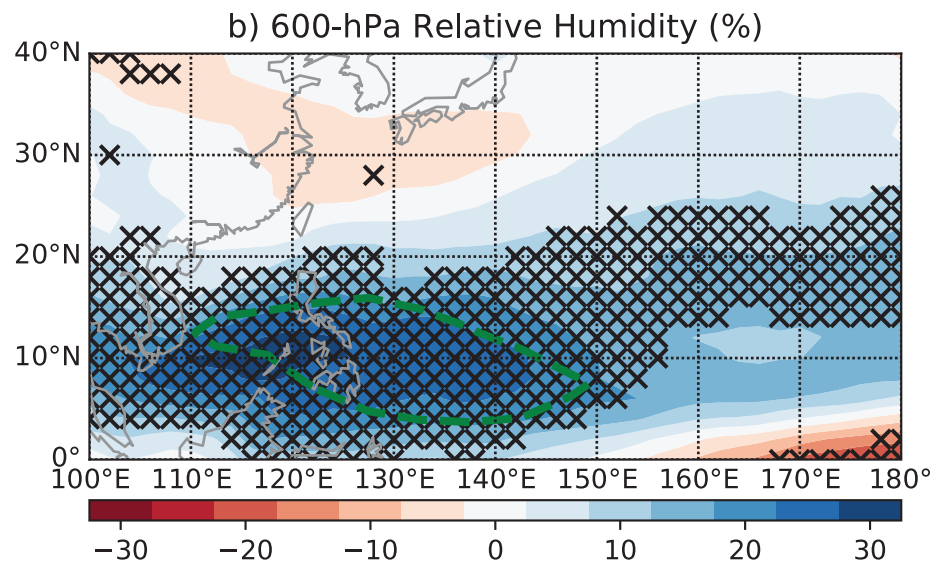
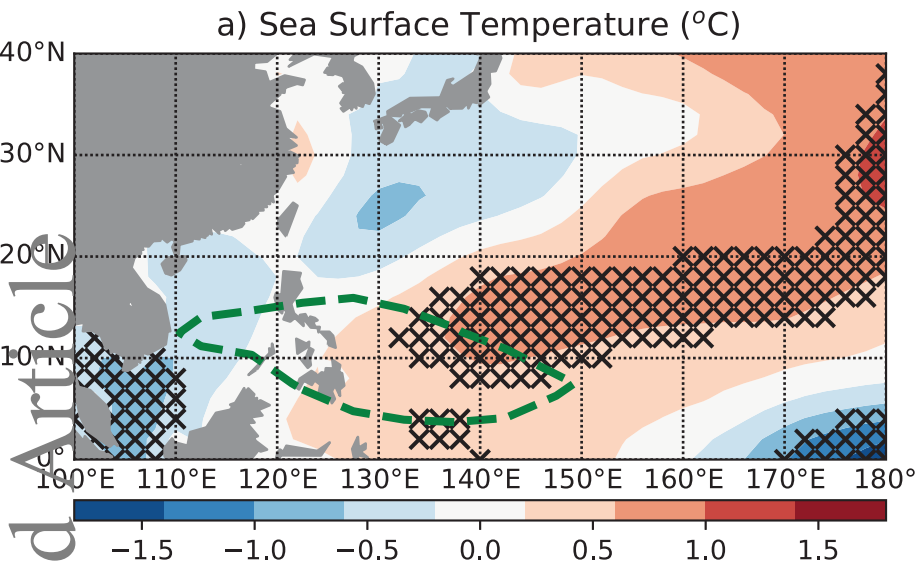
**Table 1.** List of El Niño and La Niña years during the boreal spring from 1979-2018, as well as the corresponding WNP March-May TC frequency.

El Niño		La Niña	
Year	TCs	Year	TCs
1983	0	1985	1
1987	1	1989	3
1992	0	1999	4
1993	2	2000	3
1998	0	2008	5
2010	1	2011	2
2016	0	2018	2
Mean	0.6	Mean	2.9

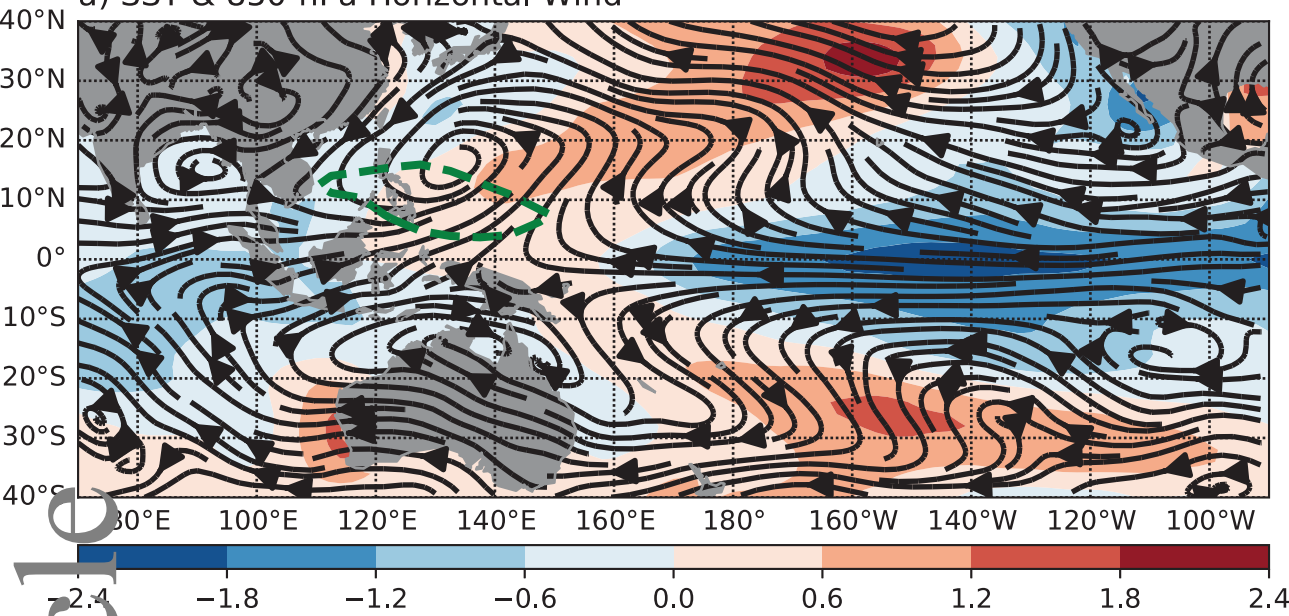




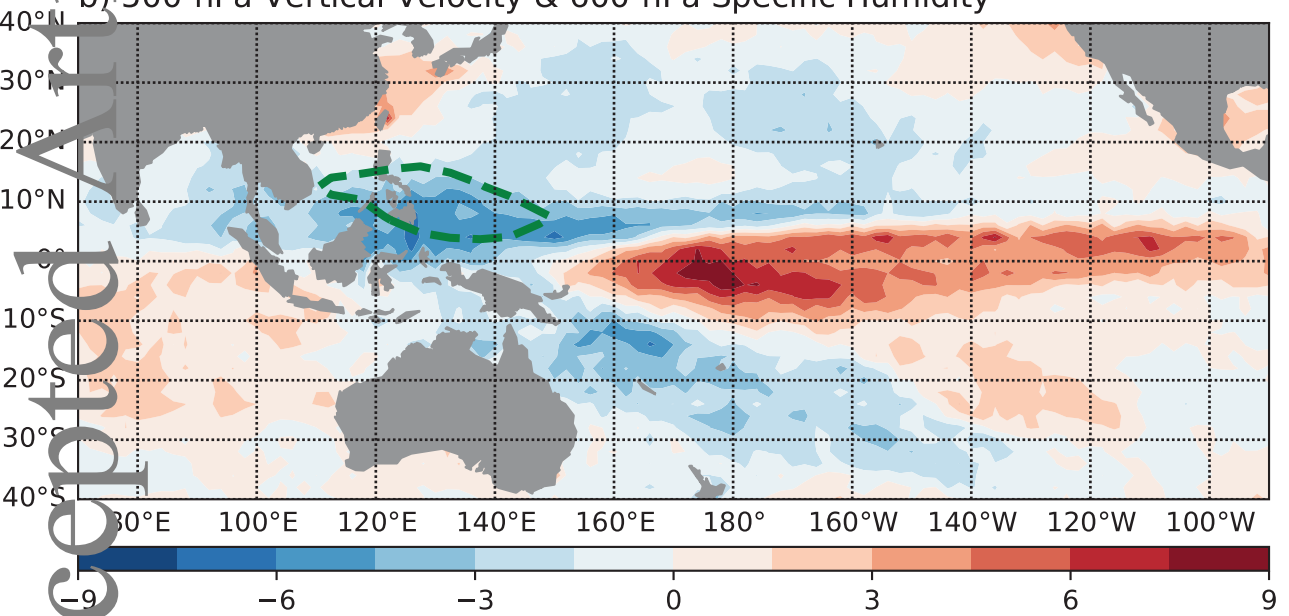
# Differences of Environmental Variables (La Niña - El Niño)



a) SST & 850-hPa Horizontal Wind



b) 500-hPa Vertical Velocity & 600-hPa Specific Humidity



c) OLR & 200-hPa Horizontal Wind

